Pergamon

Geochimica et Cosmochimica Acta, Vol. 58, No. 24, pp. 5443–5454, 1994

0016-7037/94 $6.00 + .00

0016-7037(94)00339-4

The kinetics and electrochemical rate-determining step of aqueous pyrite oxidation

MARK A. WILLIAMSON* and J. DONALD RIMSTIDT

Department of Geological Sciences, Virginia Polytechnic Institute and State University, Blacksburg, VA 24061, USA

(*Received September* 24, 1993; *accepted in revised form June* 26, 1994)

Abstract—Rate data available in the literature have been compiled for the reaction of pyrite with dissolved oxygen (DO) to produce a rate law that is applicable over four orders of magnitude in DO concentration over the pH range 2–10. The valid rate law is

$$r = 10^{-8.19(\pm 0.10)} \frac{m_{DO}^{0.5(\pm 0.04)}}{m_{H^+}^{0.11(\pm 0.01)}},$$

where r is the rate of pyrite destruction in units of mol m^{-2} s^{-1}. A series of batch and mixed flow reactor experiments were performed to determine the effect of SO_4^{2-}, Cl^-, ionic strength, and dissolved oxygen on the rate of reaction of pyrite with ferric iron. Of these, only dissolved oxygen was found to have any appreciable effect. Experimental results of the present study were combined with kinetic data reported in the literature to formulate rate laws that are applicable over a six order of magnitude range in Fe^{3+} and Fe^{2+} concentration for the pH range ~0.5–3.0. In N_2-purged solution, the rate law is

$$r = 10^{-8.58(\pm 0.15)} \frac{m_{Fe^{3+}}^{0.30(\pm 0.02)}}{m_{Fe^{2+}}^{0.47(\pm 0.03)} m_{H^+}^{0.32(\pm 0.04)}}$$

and when dissolved oxygen is present,

$$r = 10^{-6.07(\pm 0.57)} \frac{m_{Fe^{3+}}^{0.93(\pm 0.07)}}{m_{Fe^{2+}}^{0.40(\pm 0.06)}},$$

where r is the rate of pyrite destruction in mol m^{-2} s^{-1}.

Experiments were also performed in which a single pyrite sample was repeatedly reacted with ferric iron solutions of the same composition and identical surface area to mass of solution ratio (A/M). For each subsequent experiment, the rate of reaction slowed and the original behavior of the pyrite could not be reestablished by washing the pyrite with concentrated HNO_3 or EDTA. This behavior was interpreted as representative of a change in the electrochemical properties of the solid pyrite. Pretreating pyrite samples with aqueous solutions of ferrous iron and EDTA did not change the reaction rate with ferric iron; however, pretreatment with hydroxylamine hydrochloride lowered the rate significantly.

The data presented are best modeled by a nonsite-specific Freundlich multilayer isotherm. Good correlation was found between Eh and rate for the aqueous oxidation of pyrite with DO and ferric iron. Because the fractional orders of reaction are difficult to explain with a purely molecular-based mechanism, a cathodic-anodic electrochemical mechanism is favored to explain the transfer of the electron from pyrite to the aqueous oxidant.

Mechanistically, the results of this study suggest a nonsite specific interaction between dissolved oxidants and the pyrite surface. Rate correlates strongly with Eh (Fe^{3+}/Fe^{2+} ratio or DO concentration) and is consistent with an electrochemical mechanism where anodic and cathodic reactions occur at different places on the pyrite surface.

INTRODUCTION

THE MECHANISM OF A chemical or geochemical reaction, that is the detailed manner in which it proceeds, particularly the number and nature of steps involved, is a product of our imagination. A correct mechanism cannot ever be proven, but a substantial amount of information may be gathered to test any hypothesized molecular processes (WILKINS, 1974). The chemical data which are typically gathered enroute to establishing acceptable mechanisms include (1) determination of species which influence the rate of reaction with subsequent formulation of a rate law, (2) the nature of the reaction products, and (3) intermediates, (4) activation parameters (i.e., activation energy, E_a), (5) bond cleavage, and (6) linear free energy relationships (the dependance of rate on free energy of reaction).

Because of its importance in the formation of acid mine drainage, in hydrometallurgy, and in the geochemical cycling of sulfur and iron, the kinetics and mechanism of the aqueous oxidation of pyrite by ferric iron and molecular oxygen have received a great deal of attention. These two reactions are

$$FeS_2 + 14Fe^{3+} + 8H_2O \rightarrow 15Fe^{2+} + 2SO_4^{2-} + 16H^+ \quad (1)$$

and

$$FeS_2 + {}^7/_2O_2 + H_2O \rightarrow Fe^{2+} + 2SO_4^{2-} + 2H^+. \quad (2)$$

Studies of the aqueous oxidation of pyrite by dissolved oxygen and ferric iron prior to 1982 are summarized by HISKEY and

* *Present address:* Adrian Brown Consultants, Inc., 155 S. Madison St., Denver, CO 80209, USA.

SCHLITT (1982) and LOWSON (1982). Since the publication of these two review papers, GOLDHABER (1983), WIERSMA and RIMSTIDT (1984), MCKIBBEN and BARNES (1986), MOSES et al. (1987), NICHOLSON et al. (1988), and MOSES and HERMAN (1991) have contributed to our understanding of these important reactions. There is general agreement that the E_a for Eqns. 1 and 2 are high enough (on the order of 50–80 kJ mol^{-1}) to support a chemical rather than physical (i.e., diffusional) control of the rate limiting step. REEDY et al. (1991) provided important insight into bond cleavage by demonstrating that over the pH range 1–7 virtually all oxygen in the product sulfate is derived from water. GOLDHABER (1983) and MOSES et al. (1987) showed that aqueous sulfoxy intermediates could be produced during oxidation of pyrite with dissolved oxygen (DO), with the latter study demonstrating that the rate of formation of these intermediates is negligible relative to the rate of sulfate production for pH < 7. This conclusion was also noted to be true for oxidation by ferric iron. However, despite the apparent active research, many factors remain to be reconciled among the various efforts regarding the solution species which influence the rate of reaction, the nature of sulfur intermediates, and the mechanism by which these intermediates produce the eventual reaction products.

To formulate a rate law that accurately describes the rate of reaction and provides useful mechanistic information, the effect of species commonly found in the reaction system on the rate of reaction must be quantified. For example, there are several reports that the rates of oxidation of sulfide minerals by ferric iron are greater in chloride-rich solutions than in sulfate-rich solutions (e.g., chalcopyrite: DUTRIZAC, 1982; GERLACH et al., 1973; galena: WARREN et al., 1987; FUERSTENAU et al., 1986; cubanite: DUTRIZAC et al., 1970). Sulfate ions could inhibit the rate-limiting step of the oxidation reaction or chloride ions could catalyze it. Additionally, while some studies of the reaction of ferric iron with pyrite were conducted in oxygen-free environments (SMITH et al., 1970; MCKIBBEN, 1984; MOSES et al., 1987; MOSES and HERMAN, 1991) to isolate the effect of ferric iron, the weathering environment often contains oxygen. KING and LEWIS (1980) reported that the oxidation reaction with ferric iron proceeds faster in the presence of DO.

The goal of this paper is to present results of our studies on the effect of sulfate (SO_4^{2-}), chloride (Cl^-), ionic strength (I), and DO on the rate of pyrite oxidation by ferric iron, and to compile available data for the kinetics of the aqueous oxidation of pyrite. We have compiled rate data available in the literature, transformed the data to consistent units, and formulated empirical rate laws for the ferric iron and DO oxidation at 25°C. Our experiments with mixed ferric iron/DO solutions show that the mechanism of Eqn. 1 changes when DO is present compared to N_2-purged systems studied previously. The rate laws we have formulated are applicable over a wider range of solution composition than has previously been available.

METHODS

Experimental

Measurements were performed in either a mixed flow reactor (MFR; RIMSTIDT and DOVE, 1986) or a simple, stirred, batch reactor (BR; Fig. 1). The pyrite used in all experiments is from Peru and

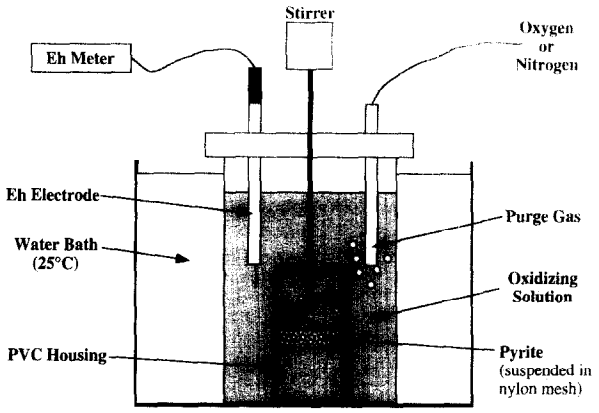

FIG. 1. A schematic diagram of the reaction kettle used for batch and mixed flow experiments in this study.

was obtained from Geoscience Resources. The material was hand sorted, immersed in 1N hydrochloric acid overnight to remove carbonate and oxide phase impurities, and air dried in an oven at 40°C. Next the pyrite was crushed and the particles ranging in size from 150 to 250 μm were recovered by sieving. This size fraction was rinsed in acetone several times to remove any fine particles adhering to the surface of the larger grains. The specific surface area of the unreacted mineral grains was determined by N_2 adsorption to be 0.047 ± 0.002 m^2 g^{-1}.

Ferric chloride run solutions were prepared by mixing aliquots of an acidified 0.5 molal ferric chloride solution into distilled water and adjusting to a final pH (<3) using reagent grade HCl. Similarly, ferric sulfate run solutions were prepared by using aliquots of an acidified 0.25 molal ferric sulfate stock solution and were acidified using reagent grade H_2SO_4. Appropriate amounts of sodium chloride and sodium sulfate were added directly to 0.0001 molal ferric chloride solutions to attain the desired Cl^- and SO_4^{2-} concentrations for investigating the effect of the anions on the rate of reaction. The pH was checked prior to each experiment with the MFR and was monitored continuously in the BR studies.

Approximately 2 g of pyrite were used for each experiment. All MFR experiments were performed using ambient air-saturated solutions. BR experiments were performed using either pure N_2 or O_2 purged solutions, with the appropriate gas bubbled through them during the course of an experiment. The Eh of reactor solutions was continuously monitored using a Fisher Scientific combination Pt 4 molal KCl/Ag-AgCl Eh electrode and an Orion Research 811 meter. For MFR experiments, the reaction was stopped when steady-state conditions were reached and the difference between the concentration of ferric iron in the feed and effluent solutions at this time was used to calculate the reaction rate. For BR experiments, the Eh of the reacting solutions was monitored continuously and the ferrous and ferric iron concentrations in the solutions was calculated from Eh readings at selected intervals. The rate of reaction for BR experiments was determined by using the b-term from a second order polynomial fit to ferric iron concentration-time data (MCKIBBEN and BARNES, 1986; RIMSTIDT and NEWCOMB, 1992).

The pyrite sample from MFR experiments was removed from the reactor, rinsed in distilled deionized water, dried in an oven at 40°C, and stored in air tight containers. Finally, the specific surface area of the reacted pyrite grains was determined from a three point N_2 BET isotherm using a Quantasorb Surface Area Analyzer. Approximately 0.2 g of four different run samples was outgassed at 50°C for five days before performing the surface area measurement. The specific surface area of the reacted pyrite samples was 0.051 ± 0.009 m^2 g^{-1}; the specific surface area of the reacted grains was essentially the same as the unreacted grains within the precision of the measurement. No surface area measurement was taken for pyrite used in BR experiments after reaction.

The concentrations of ferric and ferrous iron in the reaction solutions were calculated from the measured Eh and by simultaneously solving the Nernst equation, a mass balance equation, and equations

relating the activity to concentration. The details of this approach are described in WIERSMA (1982) and WIERSMA and RIMSTIDT (1984). The electrode was calibrated using a ZoBell's solution (NORDSTROM, 1977). A FORTRAN program which takes into account sulfate, chloride, and hydroxide ion pairing (WIERSMA, 1982) was used to calculate the activity coefficients of ferric and ferrous iron in the effluent solution. Hence, the ferric and ferrous iron concentration in reaction solutions could be calculated from its Eh.

For MFR experiments, the difference in ferric iron concentration between the feed and effluent solutions was combined with the flow rate to compute the apparent rate of the oxidation of pyrite:

$$r' = (dn/dt)_{rxn} = [(n/M)_{in} - (n/M)_{out}][dM/dt]$$
$$= (dn/dM)(dM/dt), \quad (3)$$

where $r' = (dn/dt)$ is the rate of reduction of ferric iron in this experiment, $(n/M)_{in}$ is the concentration of ferric iron of the feed solution, $(n/M)_{out}$ is the ferric iron concentration of the effluent solution, and (dM/dt) is the flow rate of solution through the reactor. The surface area and total mass of the sample were used to adjust the reaction rate to that of a standard system with 1 m^2 surface area of pyrite.

A simple plug flow reactor (PFR) was used to evaluate the effect of addition of Ag^+, SO_3^{2-}, and formaldehyde on the rate of aqueous sulfoxy anion production during oxidation by ferric iron at pH = 2. Details concerning the use of a PFR to study pyrite oxidation by ferric iron is summarized by RIMSTIDT and NEWCOMB (1992). Nitrogen-purged ferric iron solutions containing either Ag^+, SO_3^{2-}, or formaldehyde were pumped through the PFR at different rates. The addition of Ag^+ was designed to complex and thus trap any thiosulfate ($S_2O_3^{2-}$) that might be released to solution during reaction and extend its lifetime in solution so as to enable its detection. LUTTRELL and YOON (1984) suggested polysulfides could be produced on the surface of an oxidizing sulfide. Accordingly, sulfite was added to cleave, via nucleophilic attack, any polysulfides (S_n^{2-}) which might form on the surface of the mineral and release $S_2O_3^{2-}$ to solution. Addition of formaldehyde will complex any SO_3^{2-} produced and stabilize it in solution (MOSES et al., 1987). These additives were used in separate experiments and not together. Solutions which flowed out of the PFR were immediately analyzed for SO_4^{2-}, SO_3^{2-}, and $S_2O_3^{2-}$ with an ion chromatograph according to a procedure outlined by (SCHOONEN, 1988).

Compilation of Literature Rates

In addition to the experimental studies outlined above, we have collected rate data from a variety of sources (SMITH et al., 1970; MCKIBBEN, 1984; NICHOLSON et al., 1988; MOSES and HERMAN, 1991). All sources provided sufficient information to allow us to determine the reaction rate for a standard system of 1 m^2 surface area. Data were recast to consistent SI units so the rate of pyrite destruction expressed as mol m^{-2} s^{-1}.

These literature data were combined with the results of this investigation to produce a database representing a wide range of rates and aqueous solution compositions. This set of data was analyzed to produce rate laws for pyrite oxidation by ferric iron and dissolved oxygen over a very wide range of solution composition.

Multiple Linear Regression and Leverage Plots

Multiple linear regression analyses were performed using the statistical program JMP 2.0 for the Apple Macintosh computer, which is produced by the SAS Institute, Cary, NC, USA. In addition to reporting the coefficients for all independent variables in a regression, this program produces leverage plots, which are discussed in detail by SALL (1990).

In effect, a leverage plot graphically depicts the influence of an independent variable on the overall model dependent variable. The slope of the leverage plot is numerically represented by a regression coefficient and its associated standard error. For a simple regression, one dependent and one independent variable, points on a leverage plot for simple regression are actual data coordinates. On a leverage plot for a model that incorporates multiple effects (more than one independent variable), the points are no longer actual data values (see SALL, 1990). However, the intuitive interpretation of the plot is the same for multiple linear regression as for simple linear regression. A horizontal graph on a leverage plot indicates that the regressor does not significantly influence the dependent variable. Hence, the slope of a leverage plot is numerically equal to the coefficient normally associated with multiple linear regression. Leverage plots are useful for graphically displaying the effect of regressor on the dependent variable and portray in a glance which regressors are significant and which are not.

RESULTS

Compiled data for the oxidation of pyrite by DO are found in Table 1. Multiple linear regression of these data produced the rate law

$$r = 10^{-8.19(\pm 0.10)} \frac{m_{DO}^{0.5(\pm 0.04)}}{m_{H^+}^{0.11(\pm 0.01)}}, \quad (4)$$

where r is the rate of pyrite destruction in mol m^{-2} s^{-1}. The result of this regression is illustrated in Fig. 2 (numerically in Table 4) which shows a slight discrepancy between the data of SMITH et al. (1970) and MCKIBBEN (1984). This difference is about a half an order of magnitude or less at the lowest DO concentration studied by MCKIBBEN (1984). This analysis confirms a reaction order for dissolved oxygen of 0.5, consistent with MCKIBBEN and BARNES (1986) and many previous studies (see reviews by HISKEY and SCHLITT, 1982, and LOWSON, 1982). Although, MCKIBBEN and BARNES (1986) report that the rate is independent of pH, our results indicate an order of 0.11 (±0.01) which cannot be interpreted as an order of zero within the error limits of the regression. Figure 5 shows that the residuals for the model show no pronounced systematic error.

Results for our MFR and BR studies of the reaction of ferric iron and pyrite in the presence of oxygen are found in Table 2. Multiple linear regression of these data revealed that the reaction between ferric iron and pyrite is independent of the concentration of sulfate, chloride, and ionic strength (I). As illustrated in the leverage plots of Fig. 3 (numerically in Table 4), SO_4^{2-}, Cl^-, H^+, and I exert no statistically significant influence on the rate of pyrite oxidation by ferric iron in the presence of oxygen. Although the experiments represented in Table 2 and Fig. 3 were performed under partial pressures of O_2 of ambient air and under pure O_2, no difference could be discerned between the two datasets (see leverage plot for DO in Fig. 3). When DO is present, the rate of oxidation is appreciably affected by ferrous and ferric iron only and the applicable rate law is

$$r = 10^{-6.07(\pm 0.57)} \frac{m_{Fe^{3+}}^{0.93(\pm 0.07)}}{m_{Fe^{2+}}^{0.40(\pm 0.06)}}. \quad (5)$$

SMITH et al. (1970) noted a slight difference in the rate of reaction when using ferric chloride instead of ferric sulfate as the oxidant, but did not specifically quantify the effect. Unfortunately, it was not possible for us to incorporate the data of SMITH et al. (1970) for chloride and sulfate additions into the present dataset as those authors did not provide sufficient detail in their report to satisfactorily correlate tabulated rates with solution composition. SMITH et al. (1970) studied the effect of Cl^- and SO_4^{2-} over a half an order of magnitude variation in concentration, whereas the present study reports

Table 1. Data for the oxidation of pyrite by DO. The rate of pyrite destruction has units of $m^{-2}s^{-1}$ and concentration, mol kg^{-1}.

log r	log m_{O2}	log m_{H^+}	Ref	log r	log m_{O2}	log m_{H^+}	Ref
-9.13	-2.24	-2.00	1	-9.94	-3.61	-2.00	1
-9.00	-2.05	-2.00	1	-10.05	-3.79	-2.00	1
-9.64	-2.90	-2.00	1	-9.28	-2.90	-1.50	1
-9.13	-2.24	-2.00	1	-9.26	-2.90	-2.00	1
-8.80	-1.71	-2.00	1	-9.10	-2.90	-4.00	1
-9.14	-2.24	-2.00	1	-8.99	-2.90	-6.00	1
-9.15	-2.24	-2.00	1	-8.98	-2.90	-6.00	1
-9.13	-2.24	-2.00	1	-8.87	-2.90	-7.00	1
-9.05	-2.05	-2.00	1	-8.71	-2.90	-8.00	1
-8.88	-1.84	-2.00	1	-8.55	-2.90	-9.00	1
-9.13	-2.24	-2.00	1	-8.48	-2.90	-10.00	1
-8.90	-1.93	-2.00	1	-9.23	-2.94	-1.89	2
-8.75	-1.71	-2.00	1	-9.19	-2.94	-2.33	2
-9.39	-2.43	-2.00	1	-9.29	-2.94	-2.94	2
-9.28	-2.35	-2.00	1	-9.31	-2.94	-3.85	2
-9.13	-2.24	-2.00	1	-9.57	-3.63	-1.89	2
-9.45	-2.97	-2.00	1	-9.42	-3.63	-1.89	2
-9.23	-2.53	-2.00	1	-9.19	-2.86	-1.89	2
-9.24	-2.56	-2.00	1	-9.25	-2.99	-1.89	2
-9.25	-2.56	-2.00	1	-9.03	-2.94	-7.00	3
-9.29	-2.64	-2.00	1	-9.02	-2.94	-7.00	3
-9.41	-2.83	-2.00	1	-9.03	-2.94	-7.00	3
-9.61	-3.11	-2.00	1	-9.00	-2.94	-6.00	3
-9.65	-3.22	-2.00	1	-10.54	-6.14	-7.5	4
-9.73	-3.34	-2.00	1	-10.24	-5.77	-7.5	4
-9.85	-3.46	-2.00	1	-9.70	-4.92	-7.5	4
-9.88	-3.49	-2.00	1	-9.39	-4.23	-7.5	4
-9.92	-3.64	-2.00	1	-9.08	-3.62	-7.5	4

Reported data are from [1]Smith et al. (1970), [2]McKibben (1984), [3]Moses and Herman (1991) and [4]Nicholson, et al. (1988).

data spanning about 6 orders of magnitude. However, if the graphs of the SMITH et al. (1970) data are examined (their Fig. 27), it can be seen that only modest differences in the rate for Cl^- and SO_4^{2-} solutions are indicated. Additionally, they consider only two concentrations of both Cl^- and SO_4^{2-}, and this is not a significant range of variation. By performing a series of experiments using a wide range of Cl^- and SO_4^{2-} concentrations, we have been able to produce a reliable basis for evaluating the effect of these species at 25°C and atmospheric pressure. No significant systematic error was found for the model regression (Fig. 5).

Our results and data compiled from the literature for the reaction of ferric iron and pyrite in N_2-purged solutions are summarized in Table 3. Analysis of these data reveals distinctly different behavior from experiments performed in the presence of DO (Fig. 4; Table 4). For these experiments, the applicable rate law is

$$r = 10^{-8.58(\pm 0.15)} \frac{m_{Fe^{3+}}^{0.30(\pm 0.02)}}{m_{Fe^{2+}}^{0.47(\pm 0.03)} m_{H^+}^{0.32(\pm 0.04)}}. \quad (6)$$

Similar to the experiments with oxygen present, the rate is dependent on Fe^{3+} and Fe^{2+} concentrations. However, in the

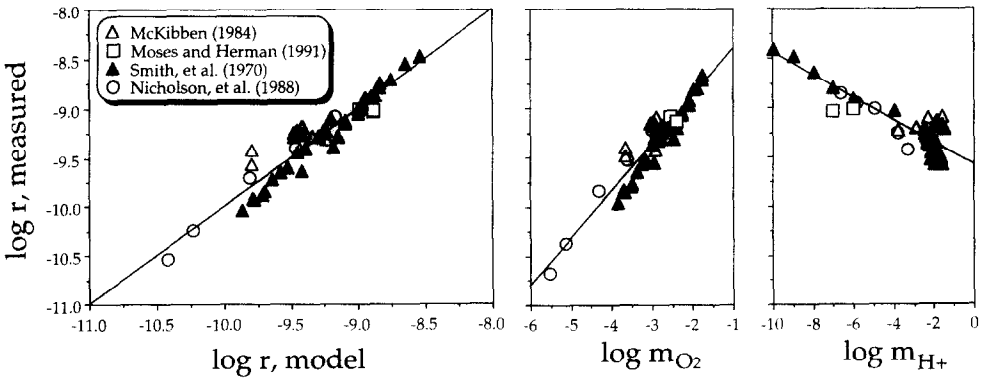

FIG. 2. Whole-model and leverage plots for multiple linear regression analysis of rate data for the aqueous oxidation of pyrite by dissolved oxygen.

Table 2. Experimental rate data from this study for the oxidation of pyrite with ferric iron in the presence of DO. Rate of destruction of pyrite is expressed as mol $m^{-2}s^{-1}$ and concentration as mol kg^{-1}.

log r	log $m_{Fe^{3+}}$	log $m_{Fe^{2+}}$	Eh	log m_{H^+}	log $m_{SO_4^{2-}}$	log m_{Cl^-}	I	Note
-7.58	-4.58	-5.30	0.813	-2.05	-10.00	-4.10	0.00908	1
-7.59	-4.07	-4.84	0.815	-1.84	-10.00	-3.59	0.01499	1
-6.90	-3.57	-4.30	0.812	-2.06	-10.00	-3.09	0.01043	1
-7.11	-3.54	-4.54	0.829	-2.06	-10.00	-3.06	0.01050	1
-6.60	-3.01	-4.69	0.869	-2.13	-10.00	-2.53	0.01332	1
-6.20	-2.51	-3.87	0.849	-2.03	-10.00	-2.03	0.02814	1
-6.36	-2.51	-4.08	0.862	-2.06	-10.00	-2.03	0.02742	1
-6.51	-3.08	-5.55	0.917	-2.53	-10.00	-2.60	0.00794	1
-6.31	-2.78	-4.14	0.851	-2.39	-10.00	-2.31	0.01411	1
-6.55	-2.61	-4.01	0.854	-2.35	-10.00	-2.13	0.01939	1
-7.14	-4.24	-5.95	0.871	-1.57	-10.00	-3.77	0.02726	1
-7.14	-3.98	-4.55	0.805	-1.57	-10.00	-3.50	0.02761	1
-7.68	-3.73	-4.33	0.807	-1.57	-10.00	-3.25	0.02813	1
-7.68	-3.57	-2.76	-	-2.00	-2.54	-10.00	0.02500	2
-7.82	-3.44	-2.79	-	-2.00	-2.54	-10.00	0.02500	2
-8.63	-4.72	-3.74	-	-1.79	-3.52	-10.00	0.01772	2
-8.67	-4.77	-3.74	-	-1.79	-3.52	-10.00	0.01772	2
-8.19	-4.04	-3.26	-	-1.97	-3.02	-10.00	0.01552	2
-9.11	-5.48	-4.22	-	-1.75	-3.02	-10.00	0.01826	2
-8.67	-4.59	-3.76	-	-1.75	-2.52	-1.00	0.12000	2
-8.65	-4.72	-3.74	-	-1.50	-2.52	0.00	1.00000	2
-8.64	-4.77	-3.74	-	-1.90	-2.52	-2.00	0.01200	2
-8.67	-4.63	-3.75	-	-1.82	-2.52	-1.00	0.12000	2
-8.63	-4.72	-3.74	-	-1.95	-2.52	0.00	1.00000	2
-8.57	-5.27	-3.71	-	-2.10	0.01	-10.00	3.00000	2
-7.78	-3.73	-3.09	-	-1.92	-10.00	-1.82	0.01802	2
-8.72	-4.89	-4.06	-	-1.94	-10.00	-1.92	0.01208	2
-8.22	-4.15	-3.60	-	-1.95	-10.00	-1.92	0.01314	2
-7.41	-2.94	-2.69	-	-1.98	-10.00	-1.82	0.02967	2
-8.55	-5.24	-3.71	-	-1.90	-0.96	-10.00	0.30200	2
-8.60	-4.92	-3.73	-	-2.10	-1.98	-10.00	0.03200	2

[1] Batch reactor [2] Mixed flow reactor.

absence of oxygen, the pH of the solution has a significant effect on the rate, consistent with the findings of McKibben and Barnes (1986). As with the other regressions, analysis of residuals does not reveal any pronounced systematic error in the analysis, hence, all error is random (Fig. 5).

The positive correlation with Fe^{3+} and negative correlation with Fe^{2+} suggests a correlation of rate with the Eh of the experimental solutions. Table 4 reports the results of a multiple linear regression model of log r as a function of Eh and log m_{H^+}, which show that the kinetics of the reaction of pyrite with ferric iron are strongly influenced by the Eh of the solution. For cases where DO was present,

$$r = 10^{-19.71(\pm 0.86)}\mathrm{Eh}^{12.93(\pm 1.04)}\mathrm{pH}^{1.0(\pm 0.29)}, \quad (7)$$

and for N_2-purged solutions

$$r = 10^{-12.7(\pm 0.11)}\mathrm{Eh}^{6.10(\pm 0.19)}\mathrm{pH}^{0.37(\pm 0.04)}. \quad (8)$$

This result was first presented by Garrels and Thompson (1960), and is consistent with an electrochemical mechanism for the reaction. This relationship is of course only valid for aqueous systems in which the E_H of the solution is in equilibrium with a reversible redox couple. Ball and Nordstrom (1985) have shown that the ratio of ferric to ferrous iron activities is representative of measured E_H in surface waters impacted by acid mine drainage in California and Davis and Ashenberg (1989) have shown a similar relationship for the Berkeley Pit in Butte, Montana, USA. Thus, for systems which have more advance stages of development of acid mine drainage, field-determined E_H and pH can be used to reliably estimate the rate of pyrite oxidation.

Consistent with McKibben (1984), who reported the rate of sulfate production to be stoichiometrically equivalent to ferrous iron production, we found that only sulfate is produced in significant quantities during pyrite oxidation with ferric iron. The PFR experiments with sulfite and formaldehyde added did not affect the rate of production of sulfate. Therefore, we do not believe that aqueous polysulfides or sulfite species are involved in the production of sulfate. When Ag^+ was added to reaction solutions, a small amount of thiosulfate, $S_2O_3^{2-}$ was detected, but was not abundant enough to be a significant intermediate for sulfate production.

DISCUSSION

Pyrite Oxidation by Dissolved Oxygen

Because Moses (1982) and Goldhaber (1983) reported the formation of aqueous sulfur intermediates at pH 6 during the reaction of pyrite with DO, McKibben and Barnes

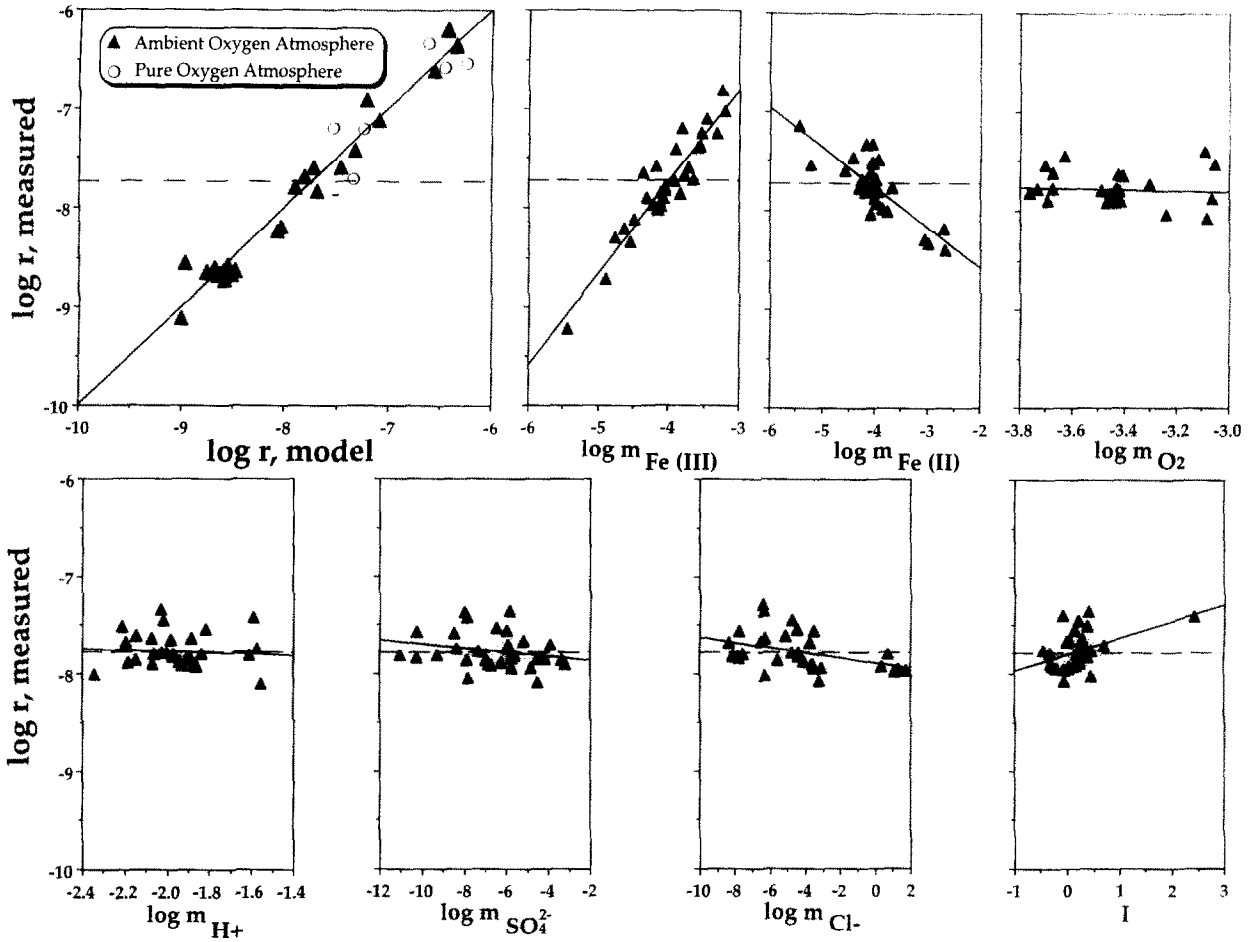

FIG. 3. Whole-model and leverage plots for multiple linear regression analysis of rate data for the aqueous oxidation of pyrite by ferric iron in the presence of dissolved oxygen. Note that the slopes for the leverage plots for DO, H^+, SO_4^{2-}, Cl^-, and I are nearly zero indicating that these parameters do not significantly affect the rate of reaction.

(1986) called into question some data from SMITH et al. (1970), which assumed the stoichiometry of Eqn. 2 to be correct at all pH values. However, the data reported by MOSES et al. (1987) clearly show that the assumption of SMITH et al. (1970) is valid for the pH range ~2–8 (2.22–7.85) as the formation of sulfoxy intermediates was not observed under these conditions. At pH = 9.06, MOSES et al. (1987) showed that the rate of sulfate production is one-half the total sulfur production. Hence, only a factor of two error (0.3 log units in rate) can be expected for the SMITH et al. (1970) data of pH 9 and 10. As seen in Fig. 2, the measurements of MOSES and HERMAN (1991) are consistent with those of SMITH et al. (1970) at pH = 6–7 and clearly establish the order of reaction for H^+. However, the small reaction order of the present report for H^+ indicates that pH has a negligible effect on observed rate which increases only one order of magnitude over a nine order of magnitude change in H^+ molality.

It could be argued that the observed increase in rate with pH may be related to the oxidation of ferrous iron released from pyrite according Eqn. 2. This process would produce ferric iron which could subsequently react with pyrite according to Eqn. 1. MOSES and HERMAN (1991) present arguments for the adsorption of ferrous iron and DO, and suggest that the oxidation of adsorbed ferrous iron has a significant effect on rate at circum-neutral pH. SMITH et al. (1970) report the results of several experiments at pH = 2 with their Warburg apparatus (an externally cycled batch reactor) in which they placed amberlite cation exchange resin in-line to remove the ferrous iron produced by the reaction of pyrite with DO. They observed no difference in rate for experiments when ferrous iron was removed vs. when it was not. Therefore, at pH = 2, oxidation of ferrous iron to produce ferric iron to oxidize pyrite is not significant. It is possible that the slight break in slope of the leverage plot for log H^+ in Fig. 2, which occurs very nearly at the pH when ferrous iron oxidation increases rapidly (WILLIAMSON and RIMSTIDT, 1992; WILLIAMSON et al., 1995), is significant and supports the hypothesis that iron oxidation is important in this reaction. However, our data do not allow us to evaluate this further.

The data in this paper for the rate of oxidation of pyrite by DO are not adequately modeled using a simple, ideal Langmuir isotherm. Under Langmuir adsorption behavior, saturation of the mineral surface will occur with increasing P_{O_2}. NICHOLSON et al. (1988) presented evidence that they believe indicated such behavior and that the rate of reaction became zeroth order in DO at high DO concentrations. The

Table 3. Rate data for oxidation of pyrite with ferric iron in the absence of dissolved oxygen. Rate of pyrite destruction is mol Py $m^{-2}s^{-1}$ and concentrations are mol kg^{-1}.

log r	log $m_{Fe^{3+}}$	log $m_{Fe^{2+}}$	Eh, mV	log m_{H^+}	Note	log r	log $m_{Fe^{3+}}$	log $m_{Fe^{2+}}$	Eh, mV	log H^+	Note
-6.67	-3.83	-4.94	0.838	-1.97	1	-8.87	-5.33	-2.00	0.668	-0.50	3
-6.77	-3.52	-4.64	0.837	-1.95	1	-8.68	-3.71	-2.01	0.669	-0.50	3
-6.59	-3.15	-4.38	0.843	-1.92	1	-8.72	-3.94	-2.02	0.656	-0.50	3
-6.54	-3.08	-4.64	0.863	-1.91	1	-8.72	-4.33	-2.02	0.633	-0.50	3
-6.50	-2.78	-4.39	0.866	-1.87	1	-9.47	-6.99	-2.01	0.475	-0.50	3
-6.64	-2.63	-4.24	0.866	-1.90	1	-9.15	-6.58	-2.02	0.500	-0.50	3
-6.43	-2.52	-4.13	0.866	-1.84	1	-8.92	-6.15	-2.01	0.525	-0.50	3
-6.81	-4.21	-5.36	0.839	-1.37	1	-10.65	-9.10	-1.99	0.349	-1.00	3
-6.69	-4.49	-5.07	0.806	-2.22	1	-9.99	-8.07	-1.98	0.410	-1.00	3
-6.86	-4.45	-4.32	0.763	-2.21	1	-9.76	-7.82	-1.98	0.425	-1.00	3
-7.39	-2.72	-4.70	-	-1.15	2	-9.64	-7.68	-1.98	0.433	-1.00	3
-7.10	-2.70	-4.70	-	-1.55	2	-9.53	-7.48	-2.01	0.446	-1.00	3
-6.88	-2.71	-4.24	-	-1.89	2	-9.39	-7.23	-1.97	0.459	-1.00	3
-6.95	-2.70	-4.62	-	-2.10	2	-9.34	-7.21	-1.98	0.460	-1.00	3
-7.05	-2.71	-4.06	-	-1.70	2	-9.42	-7.21	-2.02	0.463	-1.00	3
-7.16	-2.72	-4.15	-	-1.29	2	-9.29	-7.30	-2.00	0.456	-1.00	3
-6.79	-2.41	-4.19	-	-1.89	2	-10.38	-9.13	-1.98	0.347	-2.00	3
-8.88	-7.57	-2.01	0.441	-2.50	3	-10.24	-8.86	-1.98	0.363	-2.00	3
-9.11	-4.30	-2.61	0.670	-0.50	3	-9.88	-8.49	-1.99	0.385	-2.00	3
-8.91	-3.75	-2.23	0.680	-0.50	3	-9.77	-8.20	-1.98	0.402	-2.00	3
-8.68	-2.99	-1.72	0.695	-0.50	3	-9.68	-8.05	-1.99	0.411	-2.00	3
-8.43	-6.43	-3.28	0.583	-2.00	3	-9.53	-7.97	-1.99	0.416	-2.00	3
-8.51	-5.72	-2.95	0.606	-2.00	3	-9.32	-7.81	-1.98	0.425	-2.00	3
-9.01	-3.99	-2.41	0.676	-0.50	3	-9.34	-7.66	-1.98	0.434	-2.00	3
-8.83	-3.50	-2.06	0.685	-0.50	3	-9.23	-7.48	-1.98	0.445	-2.00	3
-8.76	-3.25	-1.91	0.690	-0.50	3	-8.93	-7.43	-2.04	0.451	-2.00	3
-8.60	-2.77	-1.57	0.699	-0.50	3	-9.14	-7.68	-2.01	0.434	-2.00	3
-8.51	-2.48	-1.38	0.705	-0.50	3	-9.77	-8.39	-1.97	0.390	-2.00	3
-8.45	-5.98	-3.05	0.596	-2.00	3	-9.58	-7.97	-1.97	0.415	-2.00	3
-8.41	-6.69	-3.40	0.575	-2.00	3	-9.24	-7.50	-1.98	0.443	-2.00	3
-8.33	-5.91	-2.96	0.595	-2.00	3	-8.33	-3.40	-1.66	0.667	-2.00	3
-9.56	-7.45	-2.04	0.450	-0.50	3	-9.24	-7.59	-2.00	0.439	-2.00	3
-9.77	-7.59	-1.99	0.439	-0.50	3	-9.32	-7.62	-2.00	0.437	-2.00	3
-9.89	-7.82	-1.99	0.425	-0.50	3	-8.90	-7.24	-2.00	0.460	-2.00	3
-10.10	-8.23	-1.96	0.399	-0.50	3	-8.33	-4.25	-2.00	0.637	-2.00	3
-10.40	-8.67	-1.98	0.374	-0.50	3	-8.45	-4.49	-2.01	0.623	-2.00	3
-9.44	-7.25	-2.00	0.459	-0.50	3	-8.43	-5.01	-2.00	0.592	-2.00	3
-9.29	-7.09	-2.01	0.469	-0.50	3	-8.46	-5.37	-2.01	0.571	-2.00	3
-9.55	-7.50	-2.01	0.445	-0.50	3	-8.47	-5.76	-2.01	0.548	-2.00	3
-9.56	-7.47	-1.98	0.445	-0.50	3	-8.54	-6.16	-2.01	0.542	-2.00	3
-9.52	-8.42	-2.98	0.448	-0.50	3	-8.86	-6.98	-2.00	0.475	-2.00	3
-9.56	-7.43	-1.99	0.448	-0.50	3	-8.66	-6.57	-2.01	0.500	-2.00	3
-9.53	-7.43	-1.99	0.448	-0.50	3	-8.41	-4.49	-1.99	0.622	-2.00	3
-9.49	-7.51	-1.97	0.442	-0.50	3	-9.78	-8.76	-1.99	0.369	-2.50	3
-9.68	-7.48	-1.97	0.444	-0.50	3	-9.60	-8.55	-1.99	0.382	-2.50	3
-9.56	-7.35	-1.96	0.451	-0.50	3	-9.49	-8.33	-1.99	0.395	-2.50	3
-10.19	-8.36	-1.97	0.392	-0.50	3	-9.32	-8.04	-1.99	0.412	-2.50	3
-9.98	-7.86	-1.98	0.422	-0.50	3	-9.19	-7.87	-1.99	0.422	-2.50	3
-8.76	-4.84	-1.93	0.597	-0.50	3	-8.99	-7.47	-1.98	0.445	-2.50	3
-9.70	-7.50	-2.00	0.445	-0.50	3	-8.82	-7.34	-1.98	0.453	-2.50	3
-8.84	-5.74	-2.01	0.549	-0.50	3						

[1]Present Study, [2]McKibben (1984), [3]Smith et al. (1970).

data tabulated in Table 1 represent DO concentrations that extend to higher values than those reported by NICHOLSON et al. (1988), but do not suggest surface saturation (see leverage plot for DO in Fig. 2). Deviations from ideal, Langmuir adsorption behavior is not uncommon (LAIDLER, 1987). Alternatively, a nonideal, multilayer adsorption model can be constructed. According to this approach, the amount of a substance adsorbed, m_{sfc}, is related to the concentration m_{sol} by

$$m_{sfc} = k_F m_{sol}^n, \quad (9)$$

where k_F and n are empirical constants. This expression is known as the Freundlich isotherm (ADAMSON, 1982; LAIDLER, 1987) and, as above, can be substituted into the general

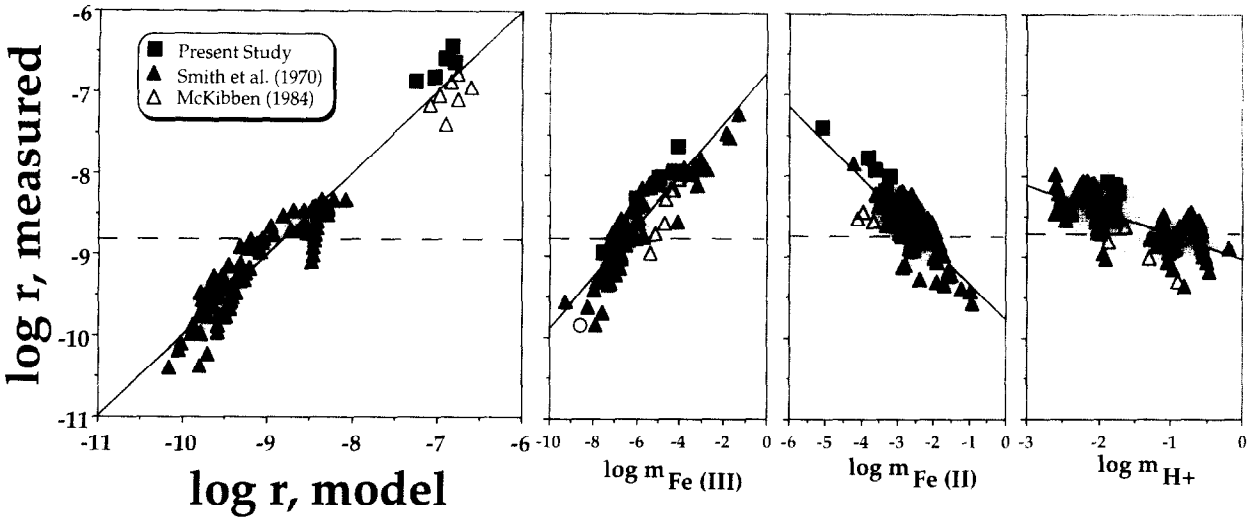

FIG. 4. Whole-model and leverage plots for multiple linear regression analysis of rate data for the aqueous oxidation of pyrite by ferric iron under an N_2 atmosphere.

form of the rate expression for rate expressed as a function of fraction of mineral surface covered by the oxidant

$$r = km_{sfc} = kk_F m''_{sol} = k' m''_{sol} \quad (10)$$

or, alternatively,

$$\log r = \log k' + n \log m_{sol}, \quad (11)$$

where k' is the apparent rate constant. As shown in Fig. 2, this relationship between log r and log m_{O_2} concentration is linear over two orders of magnitude variation in DO. It is important to note that the Freundlich isotherm does not allow saturation of the surface and that the amount of adsorbate found on the surface of the mineral, and hence rate keeps increasing with increasing DO concentration. This effect is clearly illustrated in Fig. 2. The Freundlich isotherm was developed theoretically on the basis of distributions of surface sites of different energies (see references in LAIDLER, 1987). Such behavior is consistent with the nonuniform attack of the pyrite surface by aqueous oxidants at sites of high excess surface energy as suggested by SEM studies of MCKIBBEN and BARNES (1986).

Table 4. Summary of multiple linear regression analysis to determine rates laws for pyrite oxidation by dissolved oxygen (Py/DO), ferric iron in the presence of dissolved oxygen (Py/Fe^{3+}/DO) and ferric iron in nitrogen-purged solutions (Py/Fe^{3+}/N_2).

	TERM	COEFFICIENT	STD ERROR	R^2
Py/DO				
	Intercept	-8.19	±0.10	
	log m_{O_2}	0.50	±0.04	
	log m_{H^+}	-0.11	±0.01	0.87 (n=51)
Py/Fe^{3+}/DO				
	Intercept	-6.07	±0.57	
	log $m_{Fe^{3+}}$	0.93	±0.07	
	log $m_{Fe^{2+}}$	-0.40	±0.06	
	log m_{H^+}	-0.07	±0.19	
	log $m_{SO_4^{2-}}$	-0.02	±0.02	
	log m_{Cl^-}	-0.03	±0.01	
	I	0.17	±0.07	0.96 (n=31)
	Intercept	-19.71	±0.86	
	Eh	12.93	±1.04	
	pH	1.00	±0.29	0.88 (n=31)
Py/Fe^{3+}/N_2				
	Intercept	-8.58	±0.15	
	log $m_{Fe^{3+}}$	0.30	±0.02	
	log $m_{Fe^{2+}}$	-0.47	±0.03	
	log m_{H^+}	-0.32	±0.04	0.95 (n=101)
	Intercept	-12.7	±0.11	
	Eh	6.10	±0.19	
	pH	0.37	±0.04	0.93 (n=93)

Oxidation by Ferric Iron

Our results show that the rate of reaction between Fe^{3+} and pyrite is enhanced by the presence of DO at high Fe^{3+}/Fe^{2+} ratios, but that the rate is faster in the absence of DO when Fe^{3+}/Fe^{2+} is low. Figure 6 illustrates this result by comparing the influence of Fe^{3+}/Fe^{2+} on reaction rate for a constant pH = 2 and atmospheric DO concentration versus no DO, using the rate laws presented above. Because the two trends cross, the reaction in mixed Fe^{3+}/DO systems is not simply a linear combination of the rate laws for Fe^{3+} in N_2 and for O_2 oxidations. At high Fe^{3+}/Fe^{2+}, the experimental conditions of KING and LEWIS (1980), MCKIBBEN and BARNES (1986), MOSES et al. (1987), and MOSES and HERMAN (1991), the rate is very nearly equal for the O_2-absent and O_2-present experiments. Consistent with Fig. 6, KING and LEWIS (1980) reported that the reaction rate at ambient P_{O_2} was no different than the rate under N_2. This effect also accounts for the agreement between the reports by MCKIBBEN and BARNES (1986) and RIMSTIDT and NEWCOMB (1992) which were performed under N_2 and ambient air, respectively. Significantly, in weathering environments like acid mine drainage (AMD), the Fe^{3+}/Fe^{2+} is generally much lower ($\sim 10^{-4.5}$ at pH $\sim$ 2; WILLIAMSON and RIMSTIDT, 1992; WILLIAMSON et al., 1995) than most experimental studies to date. As seen in Fig. 6, this results in rates of reaction between ferric iron and pyrite that are about two orders of magnitude slower than would be expected based on the rates laws determined in N_2-purged solutions.

Similar to the results for the oxidation of pyrite by DO, the results of this study do not support a simple, site specific

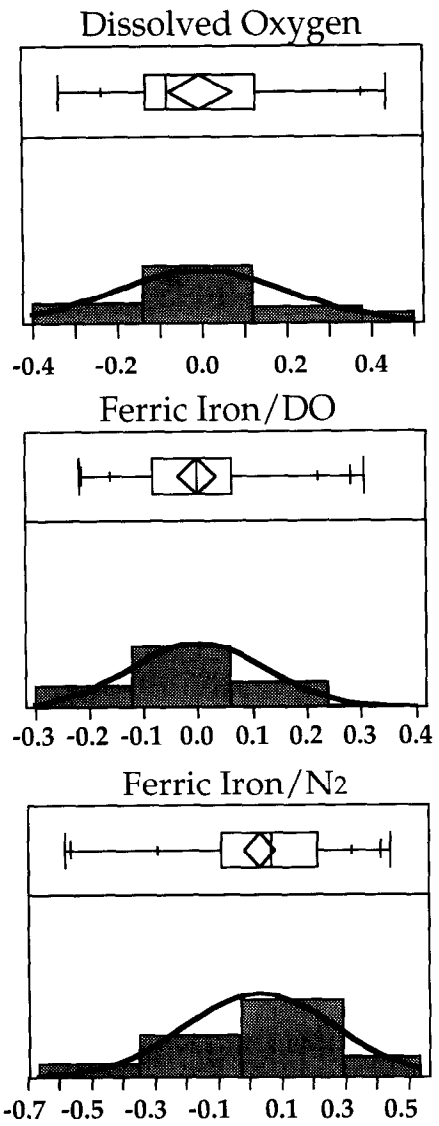

FIG. 5. Plots of whole-model residuals for regressions of Figs. 2–4. The absence of pronounced asymmetry in the distribution indicates that errors in the model fit are nearly random.

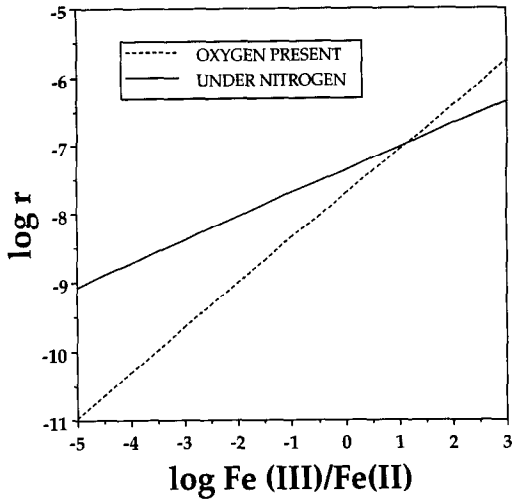

FIG. 6. Plot of log r vs. log (Fe^{3+}/Fe^{2+}) at pH = 2 for the rate of pyrite oxidation by ferric iron under a nitrogen atmosphere and in the presence of DO calculated from the regression data in Table 4. In oxygenated acid mine drainage solutions, log (Fe^{3+}/Fe^{2+}) ~ 4.5.

adsorption model to explain the kinetics of aqueous oxidation of pyrite by ferric iron. A simple Langmuir isotherm model for competitive, site-specific adsorption between Fe^{3+}, Fe^{2+}, and H^+ (to account for pH variation) produced an R^2 = 0.92. However, despite the high correlation coefficient, a plot of the residuals for the model fit shows a significant degree of asymmetry, indicative of pronounced systematic error (Fig. 7). Hence, it is difficult to place a great deal of confidence in an ideal adsorption process to explain the kinetics. Because we are able to correlate log r with log $m_{Fe^{3+}}$ and log $m_{Fe^{2+}}$ with model residuals normally distributed, we believe that a nonsite-specific Freundlich adsorbtion process may be part of the reaction mechanism.

Mechanistic Implications

Much of the difficulty in formulating a reaction mechanism for the aqueous oxidation of pyrite by DO and ferric iron is centered on whether a molecular adsorption process (effectively chemical reactions at the pyrite surface) or an electrochemical process involving distinct anodic and cathodic sites on is operative. The evidence in the present study may be used to address this dilemma and provide a convincing argument for the electrochemical mechanism.

Central to molecular mechanisms (MCKAY and HALPERN, 1959; SMITH et al., 1970; MATHEWS and ROBINS, 1974; MOSES et al., 1987; NICHOLSON et al., 1988; MOSES and HERMAN, 1991) is site-specific adsorption of the oxidant. Several studies have derived Langmuir-like relationships that appear to fit the experimental data and thus have been taken as evidence for the validity of the model. The evidence presented in this paper does not support an adsorption mechanism because saturation of the mineral surface by the oxidant cannot be demonstrated. This is particularly true for the oxidation by ferric iron where rate increases with increase in

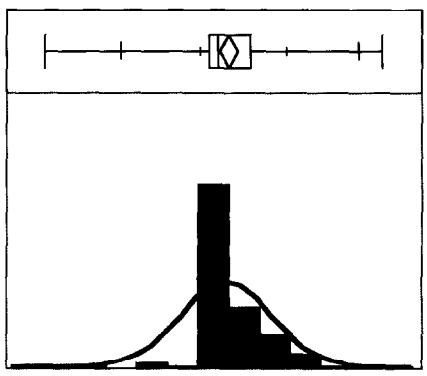

FIG. 7. Residuals from an adsorption model for the ferric iron oxidation of pyrite show a pronounced asymmetry, indicating that systematic error is present in the model and that an ideal, site-specific model of the adsorption of the oxidant onto the mineral does not explain the data.

ferric iron over a six order of magnitude range in ferric iron. Further, our efforts to model the rate of pyrite destruction by ferric iron with an adsorption model produced residuals that show pronounced asymmetry and indicate that pronounced systematic error is present in the model. However, further analysis shows that the rate of pyrite destruction can be fit with a Freundlich isotherm, which entails a multilayer, nonsite-specific process.

Fractional orders of reaction for heterogeneous reaction, such as aqueous pyrite oxidation, are often viewed as evidence for adsorption of reactants or desorption of products as rate limiting (McKIBBEN and BARNES, 1986). Our results show that the oxidation of pyrite by ferric is independent of sulfate concentration, which is the primary sulfur product (MOSES et al., 1987). This is consistent with data reported in FORNASIERO et al. (1992) indicating that above a pH of 2, pyrite has a negative surface charge. Hence, little difficulty would be encountered releasing sulfate from the surface and little interaction between the surface and negatively charged aqueous species would be anticipated. Similarly, our PFR experiments using chemical probes to track aqueous sulfur speciation showed that only a small amount of thiosulfate could be isolated when using Ag^+ as an additive. Further, no sulfite, aqueous polysulfides, or polythionates could be detected. Hence, the desorption of primary product sulfate from the pyrite surface cannot be the rate limiting step for the overall reaction. Similarly, because the rate data do not conform to a site-specific adsorption model, the adsorption of the oxidant is probably not rate limiting.

The rate of pyrite destruction is positively correlated with the concentration of the oxidant only, hence we can infer that electron transfer from the mineral to the aqueous oxidant is rate limiting. This is consistent with activation energies reported for the reaction (50–80 kJ mol^{-1}; see LOWSON, 1982, and McKIBBEN and BARNES, 1986) which indicate a chemical rather than physical barrier to reaction is rate limiting. The correlation we present between rate of mineral destruction and redox potential coupled with nonsite-specific interaction of the aqueous oxidant with the mineral is good evidence for an electrochemical mechanism involving distinct anodic and cathodic sites. Such a mechanism would conveniently account for product sulfate acquiring oxygen from the solvent water (REEDY et al., 1991) and would also account for the observed first order dependence of the reaction on water (LOWSON, 1982).

In summary, the evidence we have presented supports a reaction between pyrite and the aqueous oxidant that is an electrochemical reaction involving nonsite-specific, multilayer adsorption of the oxidant for which the electron transfer is rate limiting. Figure 8 illustrates the cathodic, rate-limiting portion of this mechanism that we feel is supported by the evidence. This mechanism does not require the oxidant to directly contact the mineral surface, but does imply that electrons from the mineral are transferred to the oxidant within a discreet zone of solvent near the mineral surface. We envision this process as somewhat analogous to an electron tunnelling process for electrodes (BOCKRIS and REDDY, 1970). The probability of finding an electron adjacent to the mineral surface decreases with distance away from the surface (e.g., its potential energy becomes greater). Similarly, the

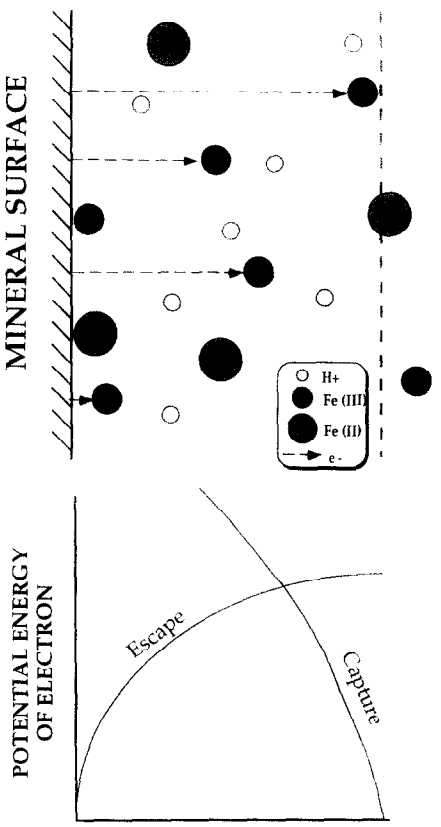

FIG. 8. This figure schematically illustrates how an electron tunnelling phenomenon may be involved at the cathodic site of an electrochemical mechanism for pyrite oxidation. Such an approach is consistent with nonideal, nonsite-specific Freundlich isotherm interaction between the mineral and the aqueous oxidant.

probability of an electron being located some position away from the aqueous oxidant decreases with an increase in distance. The potential energy maximum (really a surface in three dimensions) illustrated in Fig. 8 is the energy barrier through which an ejected electron must pass to be received by the aqueous oxidant and thereby oxidize the mineral. The passage of an electron through this energy barrier is the rate-determining step for the aqueous oxidation of pyrite, as supported by the kinetic evidence we presented earlier. This cathodic process is coupled with an as yet poorly understood anodic reaction wherein electron-deficient sulfur will react with solvent water, eventually releasing the most stable aqueous sulfur species to solution (SO_4^{2-} in the case of oxidation by ferric iron at high Eh). This interpretation is consistent with the demonstrated nonsite-specific interaction of the pyrite and the oxidant, activation energies, oxygen isotopes, and the principle of molecular economy.

Evolution of the Pyrite Surface

MOSES and HERMAN (1991) reported that the ferric iron oxidation of pyrite at pH 6–7 could not be sustained in N_2-purged solutions and that the rate of sulfate production became irreproducible after a few hundred seconds until oxygen was introduced. In this study, we observed reproducible, consistent, and smooth consumption of ferric iron in BR

experiments with ferric iron and DO mixtures. However, a detailed examination of the data revealed that a slowing of the rate occurred that cannot be attributed to consumption of oxidant in those experiments. Figure 9 is a graph of log r and log k vs. time for a BR experiment with Fe^{3+} and DO at pH = 2. Although it is reasonable to expect the rate of reaction will slow as Fe^{3+} is consumed in the closed system (which would not be regenerated to any appreciable extent by ferrous oxidation at the low pH), the rapid drop in log k over the 2225 seconds of the experiment illustrated is counter-intuitive. If the same mechanism is operative over the duration of the experiment, the value of log k should remain constant. The apparent change in log k must be due to either a corresponding change in solution composition or a change in the pyrite. This phenomenon was observed by RIMSTIDT and NEWCOMB (1992) who found that the reaction order with respect to time (n_T) was larger than the reaction order with respect to concentration (n_C). These workers concluded that an inhibitor was produced during the reaction. SATO (1992) discusses the initial change in the exact stoichiometry of the surface of a sulfide electrode so that its electrode potential is more nearly like that of the solution which it contacts. As the electrode potential nears that of the solution, the evidence reported in the present work indicates that the rate should slow.

For a series of experiments in which we re-reacted the same pyrite solids with identical solution compositions and volumes in the same BR, we are able to conclude that the ability of the pyrite to transfer charge to the aqueous oxidant changes over time. We measured the rate of ferric iron consumption for a series of six experiments. For the second, third, and fourth experiments, the pyrite was simply rinsed off between with a few milliliters of distilled-deionized water. As illustrated in Fig. 10, the rate constant dropped from one experiment to the next. Between the fourth and fifth experiment, we washed the residual pyrite in concentrated HNO_3 and, as shown in Fig. 10, were unable to recover the original kinetic behavior of the mineral. Similarly, treatment of reacted pyrite with EDTA failed to regenerate the original behavior. The infinitesimal change in surface area during this series of reactions could not account for an 85% reduction in the rate constant.

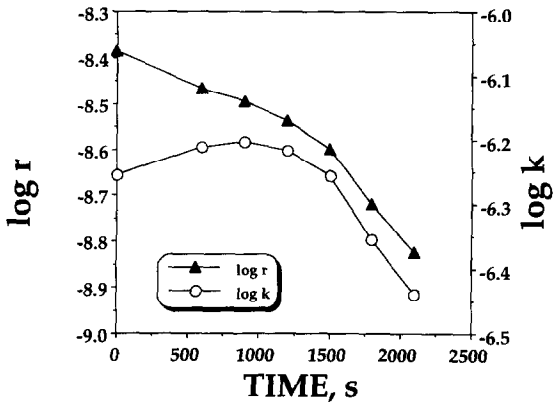

FIG. 9. A graph of log r and log k as a function of time for a single batch reactor experiment of pyrite oxidation by ferric iron in the presence of DO. The drop in the rate constant indicates a change in either the reaction mechanism or a change in the pyrite solid.

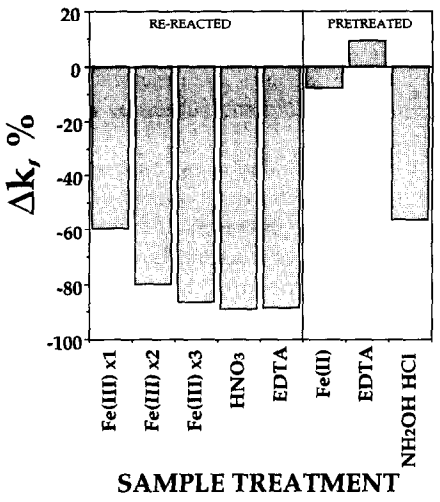

FIG. 10. This figure illustrates the drop in log k that occurs when the same pyrite sample is re-reacted with the same volume of identical composition ferric iron solution. The zero line indicates the original sample. Note that washing with concentrated HCl and EDTA is unable to restore the original behavior and indicates that a change in the pyrite sample has occurred. Pretreating pyrite with aqueous solutions of ferrous iron and EDTA does not affect the rate of reaction with ferric iron, while hydroxyamine hydrochloride ($NH_2OH \cdot HCl$) diminishes the rate.

As an extension of the experiments described above, we pretreated three pyrite samples prior to reaction with ferric iron (plus DO) with 0.4 m Fe^{2+} (pH = 1), 1 m EDTA, and 1 m $NH_2OH \cdot HCl$ (hydroxylamine hydrochloride) for 1 h, then rinsed the solids with a few milliliters of water. Pretreatment with ferrous iron and EDTA had little effect on the reaction rate (Fig. 10). However, $NH_2OH \cdot HCl$ pretreatment depressed the rate constant by 50%.

Because washing the reacted mineral grains with water, concentrated HNO_3, or EDTA failed to reproduce original rates, we are able to discount the hypothesis that the lowering of k over time is due to solution effects (i.e., adsorbtion of an inhibitor from solution). We hypothesize that a change in the electrochemical behavior of the solid has occurred. The semiconductor properties of pyrite have been reported to influence the rate of reaction in systems similar to the weathering environment (LOWSON, 1982) and may be altered by simply polishing (P. E. Richardson, pers. comm., 1992). However, the present data do not allow further interpretation.

CONCLUSIONS

We have developed rate laws for the oxidation of pyrite by molecular oxygen and ferric iron that are applicable over a wide range of solution composition. Multiple linear regression of rate data available in the literature for the reaction of pyrite with DO produced the rate law shown in Eqn. 4. The rate dependence on DO was observed not to level off over a four order of magnitude variation in DO concentration.

The rate of reaction of pyrite with ferric iron is not influenced by SO_4^{2-}, Cl^-, or I but is significantly affected by the presence of DO (but not its concentration). For N_2-purged

solutions, the applicable rate law (Eqn. 5) contrasts markedly with the rate law determined for oxygenated solutions (Eqn. 6). For these two rate laws, the order with respect to ferric iron is dramatically different, suggesting a difference in the reaction mechanism.

The rate of pyrite oxidation by ferric iron is strongly correlated with solution Eh, which underscores the importance of considering an electrochemical mechanism for the reaction. The fractional orders of reaction shown in the rate laws for the oxidation with ferric iron are difficult to interpret based strictly on a molecular mechanism. An electrochemical mechanism, involving distinct anodic and cathodic sites, which need not be proximal to each other, is consistent with the isotopic studies of REEDY et al. (1991) showing virtually all sulfate oxygen derived from water, and high E_a values which are typically well beyond that which can be expected from diffusion-controlled processes.

An important result of the work presented in this paper is the remarkable agreement between datasets from different workers. The studies from which the present report has drawn upon span 20 years and represents as many as three different investigators using at least three different experimental procedures to follow the rate of this geochemically significant reaction. This results in our ability to produce rate laws for the aqueous oxidation of pyrite by DO and ferric iron that have a significant degree of confidence.

Acknowledgments—Support for this work came from the National Science Foundation grant EAR-9004312. The authors appreciate reviews of this manuscript provided by M. A. A. Schoonen and R. V. Nicholson.

Editorial handling: E. J. Reardon

REFERENCES

ADAMSON A. W. (1982) *Physical Chemistry of Surfaces*. Wiley.

BALL J. W. and NORDSTROM D. K. (1985) *Major and trace metal analyses of acid mine waters in the Leviathan mine drainage basin, California/Nevada-October 1981 to October 1982*. U.S. Geol. Surv. Water Resourc. Invest. Rpt. 85-4169.

BOCKRIS J. O. and REDDY A. K. N. (1970) *Modern Electrochemistry*, Vol. 2. Plenum Press.

DAVIS A. and ASHENBERG D. (1989) The aqueous geochemistry of the Berkeley Pit, Butte, Montana, USA. *Appl. Geochem.* **4**, 23–36.

DUTRIZAC J. E. (1982) Ferric ion leaching of chalcopyrites from different localities. *Metal. Trans.* **13B**, 303.

DUTRIZAC J. E., MACDONALD R. J. C., and INGRAHAM T. R. (1970) The kinetics of dissolution of cubanite in aqueous acidic ferric sulfate solutions. *Metal. Trans.* **1**, 3083–3088.

FORNASIERO D., EIJT V., and RALSTON J. (1992) An electrokinetic study of pyrite oxidation. *Colloids Surf.* **62**, 63–73.

FUERSTENAU M. C., CHEN C. C., HANK N., and PALMER B. R. (1986) Kinetics of galena dissolution in ferric chloride solutions. *Metal. Trans.* **17B**, 415–423.

GARRELS R. M. and THOMPSON M. E. (1960) Oxidation of pyrite by iron sulfate solutions. *Amer. J. Sci.* **258A**, 57–67.

GERLACH J. K., GOCK E. D., and GHOSH S. K. (1973) Activation and leaching of chalcopyrite concentrates with dilute sulfuric acid. In *International Symposium on Hydrometallurgy* (ed. D. J. I. EVANS and R. S. SCHOEMAKER), pp. 403–416. AIME.

GOLDHABER M. B. (1983) Experimental study of metastable sulfur oxyanion formation during pyrite oxidation at pH 6–9 and 30°C. *Amer. J. Sci.* **283**, 193–217.

HISKEY J. B. and SCHLITT W. J. (1982) Aqueous oxidation of pyrite. Interfacing Technologies in Solution Mining. *Proceedings 2nd SME-SPE Internatl. Sol. Mining Symp., Denver CO*, pp. 55–74.

KING W. E. and LEWIS J. A. (1980) Simultaneous effects of oxygen and ferric iron on pyrite oxidation in an aqueous slurry. *Ind. Eng. Chem. Process Des. Dev.* **19**, 719–722.

LAIDLER K. J. (1987) *Chemical Kinetics*, 3rd ed. Harper and Row.

LOWSON R. T. (1982) Aqueous pyrite oxidation by molecular oxygen. *Chem. Rev.* **82**, 461–497.

LUTTRELL G. H. and YOON R.-H. (1984) Surface studies of the collectorless flotation of chalcopyrite. *Colloids Surf.* **12**, 239–254.

MATHEWS C. T. and ROBINS R. G. (1974) Aqueous oxidation of iron disulfide ny molecular oxygen. *Australian Chem. Eng.* **15**, 19–24.

MCKAY D. R. and HALPERN J. (1959) A kinetic study of the oxidation of pyrite in aqueous suspension. *AIME Trans.* **212**, 301–309.

MCKIBBEN M. A. (1984) Kinetics of aqueous oxidation of pyrite by ferric iron, oxygen and hydrogen peroxide from pH 1–4 and 20–40°C. Ph.D. thesis, Pennsylvania State Univ.

MCKIBBEN M. A. and BARNES H. L. (1986) Oxidation of pyrite in low temperature acidic solutions: rate laws and surface textures. *Geochim. Cosmochim. Acta* **50**, 1509–1520.

MOSES C. O. (1982) Kinetic investigations of sulfide mineral oxidation in sterile aqueous media. Ph.D. thesis, Univ. Virginia.

MOSES C. O. and HERMAN J. S. (1991) Pyrite oxidation at circumneutral pH. *Geochim. Cosmochim. Acta* **55**, 471–482.

MOSES C. O., NORDSTROM D. K., HERMAN J. S., and MILLS A. L. (1987) Aqueous pyrite oxidation by dissolved oxygen and by ferric iron. *Geochim. Cosmochim. Acta* **51**, 1561–1571.

NICHOLSON R. V., GILLHAM R. W., and REARDON E. J. (1988) Pyrite oxidation in carbonate-buffered solution: I. Experimental kinetics. *Geochim. Cosmochim. Acta* **52**, 1077–1085.

NORDSTROM D. K. (1977) Thermochemical redox equilibria of ZoBell's solution. *Geochim. Cosmochim. Acta* **41**, 1836–1841.

REEDY B. J., BEATTIE J. K., and LOWSON R. T. (1991) A vibrational spectroscopic ^{18}O tracer study of pyrite oxidation. *Geochim. Cosmochim. Acta* **55**, 1609–1614.

RIMSTIDT J. D. and DOVE P. M. (1986) Mineral/solution reaction rates in a mixed flow reactor: wollastonite hydrolysis. *Geochim. Cosmochim. Acta* **50**, 2509–2516.

RIMSTIDT J. D. and NEWCOMB W. D. (1992) Measurement and analysis of rate data: The rate of reaction of ferric iron with pyrite. *Geochim. Cosmochim. Acta* **57**, 1919–1934.

SALL J. (1990) Leverage plots for general linear hypotheses. *Amer. Stat.* **44**, 308–315.

SATO M. (1992) Persistency field Eh-pH diagrams for sulfides and their application to supergene oxidation and enrichment of sulfide ore bodies. *Geochim. Cosmochim. Acta* **56**, 3111–3156.

SCHOONEN M. A. A. (1988) Mechanisms of pyrite and marcasite formation from solutions between 25 and 300° celsius. Ph.D. thesis, Pennsylvania State Univ.

SMITH E. E. et al. (1970) Sulfide to sulfate reaction mechanism. *Fed. Water Qual. Admin. Water Poll. Contrl. Res. Study #14010-FPS-02-70.*

WARREN G. W., KIM S.-H., and HENEIN H. (1987) The effect of chloride ion on the ferric chloride leaching of Galena concentrate. *Metal. Trans.* **B18**, 59–65.

WIERSMA C. L. (1982) Relative rates of reaction of pyrite and marcasite with ferric iron at low pH. Masters thesis, Virginia Polytechnic Institute and State University.

WIERSMA C. L., and RIMSTIDT J. D. (1984) Rates of reaction of pyrite and marcasite with ferric iron at pH 2. *Geochim. Cosmochim. Acta* **48**, 85–92.

WILKINS R. G. (1974) *The Study of Kinetics and Mechanisms of Reactions of Transition Metal Complexes*. Allyn and Bacon.

WILLIAMSON M. A. and RIMSTIDT J. D. (1992) *Kinetics in Acid Mine Drainage; Goldschmidt Int'l. Conf. Geochim. Abstr. Prog.*

WILLIAMSON M. A., KIRBY C. S., RIMSTIDT J. D., and NORDSTROM D. K. (1995) Quantitative comparison of pyrite and iron oxidation rates in acid mine drainage: The rate-determining step. *Geochim. Cosmochim. Acta* (submitted).